Available online at www.sciencedirect.com
SciVerse ScienceDirect
Energy Procedia 28 (2012) 28 – 36
Energy Procedia

Fuel Cells 2012 Science & Technology – A Grove Fuel Cell Event

Gradual internal reforming of ethanol in solid oxide fuel cells

S.D. Nobrega[a], F.C. Fonseca[a*], P. Gelin[b], F.B. Noronha[c], S. Georges[d], M.C. Steil[d]

[a]*Insituto de Pesquisas Energéticas e Nucleares, IPEN, São Paulo, SP, 05508-000, Brazil*
[b]*Institut de recherches sur la catalyse et l'environnement de Lyon, 69626 Lyon, France*
[c]*Instituto Nacional de Tecnologia, Laboratorio de Catalise, Rio de Janeiro, RJ, 20081-312, Brazil*
[d]*Laboratoire d'Electrochimie et de Physicochimie des Matériaux et des Interfaces, 38400 Saint Martin d'Hères, France*

Abstract

Electrolyte (yttria-stabilised zirconia, YSZ) supported solid oxide fuel cells (SOFCs) were fabricated using spin coating of standard LSM cathode and Ni-YSZ cermet anode. A ceria-based catalytic layer was deposited onto the anode with a special current collector design. Such a single cell configuration allows operation by gradual internal reforming of direct carbon-containing fuels. First, the fabricated single cells were operated with hydrogen to determine the optimised conditions of fuel concentration and flow rate regarding faradaïc efficiency. Then, the fuel was switched to dry ethanol and the cells were operated for several hours (100 h) with good stability. Post-operation electron microcopy analyses revealed no carbon formation in the anode layer. The results indicate that the gradual internal reforming mechanism is effective, opening up the way to multi-fuel SOFCs, provided that a suitable catalyst layer and cell design are available.

Keywords: Ceria-based catalytic layer; Gradual internal reforming; Ethanol; Optimisation

1. Introduction

The solid oxide fuel cell (SOFC) is considered as an attractive power source in part because of its fuel flexibility, which means it can operate directly on different fuels without external reforming [1]. Hydrogen, the most widely used fuel in SOFC, is usually produced from steam reforming of hydrocarbons, and has several issues regarding its storage and distribution. If alternative fuels, such as hydrocarbons and alcohols, could be used directly, the overall energy cost would be significantly reduced [2]. Among many fuels, ethanol offers several advantages such as easy and safe storage, handling, and

*Corresponding author: Tel: +55-11-3133-9282; fax: +55-11-3133-9282.
E-mail address: fcfonseca@ipen.br

 doi:10.1016/j.egypro.2012.08.037

delivery. In addition, ethanol is a renewable derived from various biomass sources, it is readily available, less toxic than methanol, and it has a high energy density [1–3].

The commonly used SOFC anode, a cermet consisting of nickel and yttrium-stabilised zirconia (YSZ), has excellent catalytic properties and stability for the H_2 oxidation at the usual operation conditions [1, 2]. Nevertheless, the use of Ni-YSZ catalysts with carbon-containing fuels results in the deposition of large quantities of carbon on the nickel surface, resulting in a marked irreversible reduction of cell performance. Such a limitation has raised a great deal of attention for the development of carbon-resistant anodes.

Recently, it has been demonstrated that SOFCs can be operated on hydrocarbon fuels directly or through internal reforming, by simply modifying the conventional anode or adding a layer of catalyst that has high activity towards the hydrocarbon reforming reactions [4]. The carbon formation can be avoided using a support with good redox properties. Better catalytic performance with good stability and high hydrogen selectivity can be expected in supports with good redox properties [5]. Therefore, alternative materials that exhibit high catalytic activity in ethanol conversion, and adequate ionic and electronic conductivities, have been proposed as anode materials for SOFCs operating directly on dry ethanol. The use of ceria-based oxide (such as gadolinium or zirconium doped ceria) as a catalytic layer has been proposed as an approach for suppressing carbon deposition of SOFCs running on ethanol [2, 4–7]. The high oxygen storage and transport properties of CeO_2 provide high resistance to carbon deposition in ethanol reforming reactions [8].

Nonetheless, previous studies on ethanol conversion were mostly based on internal steam reforming [9, 10]. Considering the basic case of CH_4, used in Direct Internal Reforming (DIR) conditions ($[CH_4]/[H_2O] = 1$), the reaction with methane and steam occurring at the anode leads to the formation of H_2 and CO by the steam reforming reaction [11]. However, the addition of large amounts of water to the feed is required to reach the stoichiometric amount $[CH_4]/[H_2O]$, which lowers the overall yield of the cell, in particular. Moreover, in DIR, the steam reforming is likely to be localised mainly close to the inlet of the anode, causing a thermal stress induced by the endothermic nature of the reforming reaction. As an alternative to such DIR limitations, Gradual Internal Reforming (GIR) was proposed [11–14]. In GIR, the water released by the electrochemical oxidation of hydrogen at the anode is used for steam reforming of the fuel in a catalytic layer deposited over the anode. The fuel is gradually consumed producing hydrogen. The H_2 electrochemical oxidation and fuel steam reforming are then self-sustained by each other along the anodic channel. Fig. 1 depicts the principle of the cell operation by GIR associated with electrocatalytic separation (use at the same time of the best catalyst and anode) in the case of ethanol as the fuel. The feasibility of GIR operation mechanism with dry ethanol, has already been demonstrated [15].

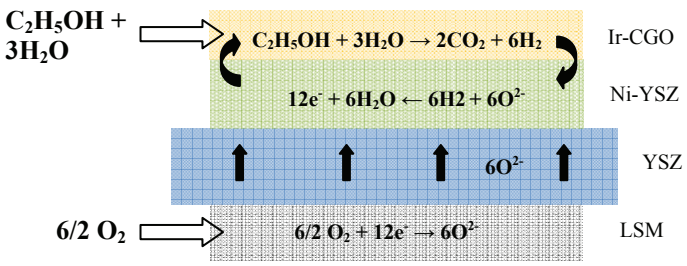

Fig. 1. Scheme of the principle of GIR associated with electrocatalytic separation. The unit cell is comprised of an LSM cathode, YSZ electrolyte, Ni-YSZ anode, and Ir-CGO catalytic layer and specific anodic collector.

In the present work, the design and stable operation for 100 h of a direct (anhydrous) ethanol SOFC with an additional ceria-based catalytic layer are described.

2. Experimental

2.1. Single cell fabrication

Electrolyte-supported single cells were fabricated for direct operation with ethanol.

2.1.1. Electrolyte preparation

Single fuel cells tested in this study were fabricated from a planar 56 mm diameter and ~1 mm thick supporting electrolyte, composed of dense yttria-stabilised (8 mol%) zirconia (YSZ) from Tosoh (Japan). The electrolyte was produced by uniaxial compression of 5 tonne cm^{-2}, followed by isostatic pressing at 2500 bar. The electrolyte was sintered for 2 h at 1450°C. To obtain accurate geometry, electrolytes supports were machined after sintering by diamond tools.

2.1.2. Cathode preparation

Strontium-doped lanthanum manganite (LSM) was used as the cathode material. The composition $La_{0.65}Sr_{0.30}MnO_3$ was synthesised by the polymeric precursor technique. In this technique, the starting materials used were $La(NO_3)_2.6(H_2O)$ (Aldrich, 99.99%), $Sr(NO_3)_3.4(H_2O)$ (Aldrich, 99%), $Mn(CH_3CO_3)_2.4(H_2O)$ (Aldrich, 99%). Citric acid (Fluka, 99.5%) was added to an aqueous solution of the metallic salts under constant mixing and heated at ~70°C. Ethylene glycol (Aldrich, 99.8%) was added, and the resulting solution was kept under constant mixing and heating (70°C) until a viscous resin was obtained. The polymeric precursor was heated at 300°C and calcined for 1 h at 800°C to obtain single-phase LSM compounds. The cathode was fabricated with two layers: the functional layer LSM-YSZ (50-50 wt%), which is an interfacial layer deposited onto the electrolyte support, and the LSM current collector layer, deposited over the functional layer. The two cathode layers were deposited using the spin-coating method, with an active area of 13.8 cm^2. The layer thickness of both the functional and current collector layer was controlled by the suspension mass deposited and the number of deposition steps on the spin-coating. The suspensions for spin-coating were developed aiming at simple preparation and fast deposition, with minimum spin-coating steps to achieve the desired layer thickness. The suspensions for spin-coating were prepared by dissolving ethyl cellulose in terpineol (Aldrich), under constant mixing and heating. After cooling to room temperature, LSM powder was added and mixed for 15 h in a ball milling apparatus with zirconia jar and balls. In the spin-coating technique, the YSZ substrate is fixed with vacuum to the spin-coater (Laurel, model WS-400-6NPP-LITE), the electrode suspension is deposited onto the substrate, and system is rotated at 6000 rpm for 10 s. After the deposition step, the deposited layer is dried in a hot plate at 80°C for 5 min. After sintering at 1150°C in air, the cathode functional and current collector layers were ~20 μm and 60 μm thick, respectively.

2.1.3. Preparation of anode

Ni-YSZ composites were prepared by a liquid mixture technique. Such a method consists in the evaporation of a dispersion of YSZ in a nickel acetate (Aldrich, 99%) solution in ethanol under mixing and heating at 70°C, followed by calcination at 450°C for 5 h [16]. The anode layers were deposited using the spin-coating method, with an active area of 13.8 cm^2. Sintering was carried out at 1400°C in air. The anode was fabricated with two layers: functional and current collector layers were Ni-YSZ (40-60 vol%) with ~20 μm thickness, and Ni-YSZ (60-40 vol%) with ~40 μm thickness, respectively. The current

collector was formed by painting with gold ink contact pads connected to a gold wire (0.5 mm diameter), which was fixed with gold ink over the anode layer forming a ring of ~42 mm diameter.

2.1.4. Preparation of catalyst layer

The Ir-containing (0.1 mol%) $Ce_{0.9}Gd_{0.1}O_{2-x}$ catalyst (Ir-CGO) was prepared by an impregnation technique. The appropriate amount of an iridium acetylacetonate (Alfa Aesar) solution in toluene was added to a suspension of CGO (Praxair, 40.9 $m^2.g^{-1}$). This suspension was maintained under stirring for 4 h at 50°C. After complete evaporation of the solvent under reduced pressure, the catalyst was dried overnight at 120°C, calcined in flowing O_2 for 6 h at 350°C [17]. The catalytic layer was deposited onto the anode by the spray-coating technique. The suspension of the catalytic layer was formulated based on catalyst powder (0.1 mol% Ir-CGO) and a pore former, in which were added PVP dispersant, PVB plasticiser, ethanol (Sigma-Aldrich, absolute) and terpineol (Fisher Scientific). After the coating step, the deposited layer was dried in an oven for 30 min at 100°C. The catalytic layer was thermally treated for 2 h at 900°C in argon.

2.2. Cell tests

Fig. 2 shows the arrangement of the cell testing apparatus. The single cell (1) was set up in a homemade test bench comprised of two alumina tubes (2) (anode and cathode side) using gold rings (0.5 mm thickness and 53 mm diameter) on both surfaces of the electrolyte for the sealing.

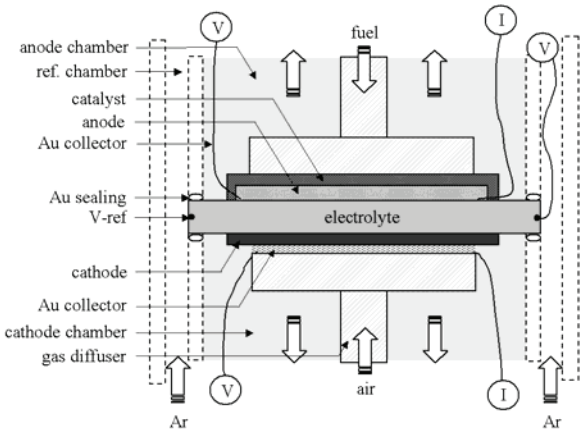

Fig. 2. Schematic representation of the experimental setup used for single cell testing.

The tubes were inserted in a vertical measurement system with a third external concentric alumina tube in which a guard atmosphere of Ar was flowed. Alumina capillaries were inserted in the concentric tubes of alumina, with gold screens at the extremity in contact with the anode and cathode of the cell. Gold wires allow the current and potential monitoring for independent current and voltage measurements. The system is closed with a metallic head and sealed with the aid of gold rings and a rubber gasket. The system has gas inlets and outlets. Fuel cell tests were initially performed at 850°C in H_2 (60%) balanced with Ar. Various flow rates and fuel concentrations were used to optimise the fuel utilisation, calculated as the faradaïc efficiency. After optimisation, steady operation in H_2 was obtained to initiate the steam release necessary to ensure the gradual internal reforming of ethanol. The fuel was then switched to ethanol. Liquid ethanol was kept in a thermal bath with controlled temperature and carried by Ar at

various flow rates. Gas flow rates were set by calibrated mass flowmeters (Brooks). Electrochemical impedance spectroscopy (EIS) and polarisation vs. time measurements were performed with an Autolab PGSTAT128N potentiostat associated with a BSTR10A current booster. A variable resistor bench connected in series with the fuel cell was used for polarisation curve measurements.

3. Results

Initially, the optmised fuel cell operation conditions were determined in hydrogen. Fig. 3 shows the optimisation of fuel utilisation (U_f, faradaïc efficiency) using H_2 balanced with Ar, varying the total fuel flow rate as a function of time. For each flow rate, H_2 contents of 30, 60 and 90% were investigated. Fuel cell testing started with a total flow of 4 L.h^{-1}, as show in Fig. 3(a). With 30% H_2, the current density (i) obtained was ~0.095 A cm^{-2}, and the H_2 utilisation U_f = 43%. Then, the amount of H_2 was increased to 60% (i ~ 0.105 A cm^{-2}) and U_f decreased to 28%. Finally, using 90% H_2, U_f decreased to 20%. The results show that by increasing the amount of H_2 to 90%, the current density is maximal; however, U_f for H_2 is minimal. Similar behaviour was observed for total flow of 3 and 2 L.h^{-1}, as shown in Fig. 3(b) and 3(c), respectively.

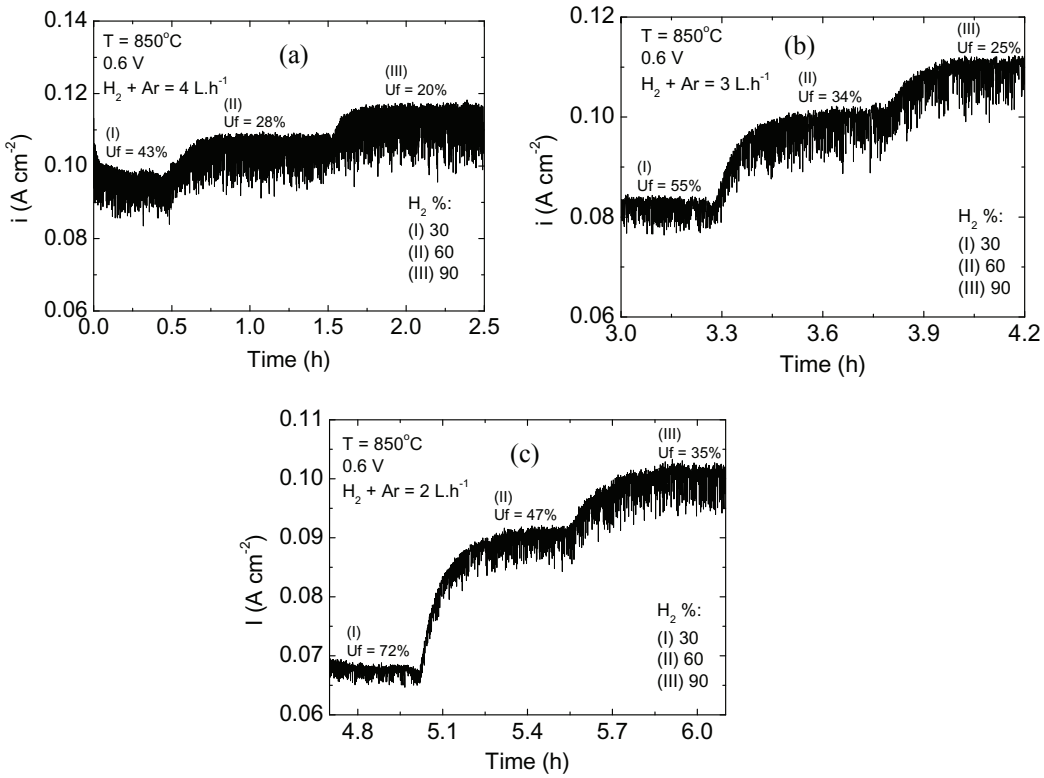

Fig. 3. Optimisation of single-cell operation in different concentrations of hydrogen at 850°C, with the total fuel flow rate of (a) 4 L.h^{-1}, (b) 3 L.h^{-1}, and (c) 2 L.h^{-1}.

Fig. 4(a) shows the current density (i) determined from Fig. 3 at 0.6 V as a function of the H_2 content. It can be observed that an equivalent i = 0.09 A.cm^{-2} is obtained with both 30% H_2 at 4 L.h^{-1} flow rate and with 60% H_2 at 2 L.h^{-1}. Accordingly, in Fig. 4(b) it is possible to observe that 60% H_2 at 4 L.h^{-1} is equivalent to 90% H_2 at 3 L.h^{-1}. Therefore, the optimised conditions for the fuel cell operation were set at 60% H_2 with 4 L.h^{-1} flow rate.

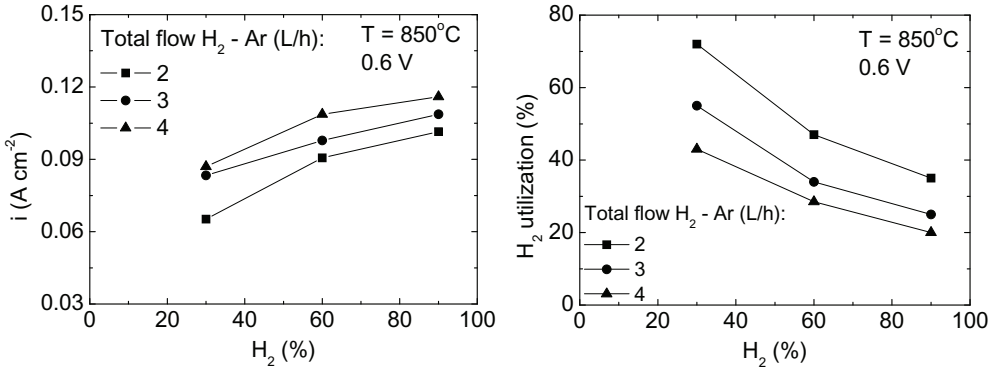

Fig. 4. (a) Current density and (b) H_2 utilisation versus the H_2 content, obtained at 850°C.

To investigate the stability of the fuel cell in dry ethanol in gradual internal reforming conditions, potentiostatic curves were recorded at 0.6 V as a function of time, as shown in Fig. 5. Tests started with 60% H_2 balanced with Ar (total flow = 2 L.h^{-1}). After steady operation in H_2 (~1 h), the fuel was balanced with ethanol and Ar, and after 0.5 h, the fuel was switched to 10% ethanol and Ar. The ethanol content was controlled by setting the temperature of the thermal bath at 29°C, in accordance with Clapeyron's law. The flow rates of both fuels were calculated to carry an equivalent theoretical number of electrons to the anode according to the simple chemical mechanisms depicted in Fig. 1 ($2e^-$ for H_2, $12e^-$ for ethanol). Fig. 5 shows stable operation of the cell for 12 h under direct ethanol, at 0.6 V and i ~ 0.9 A cm^{-2}, after initiation in H_2.

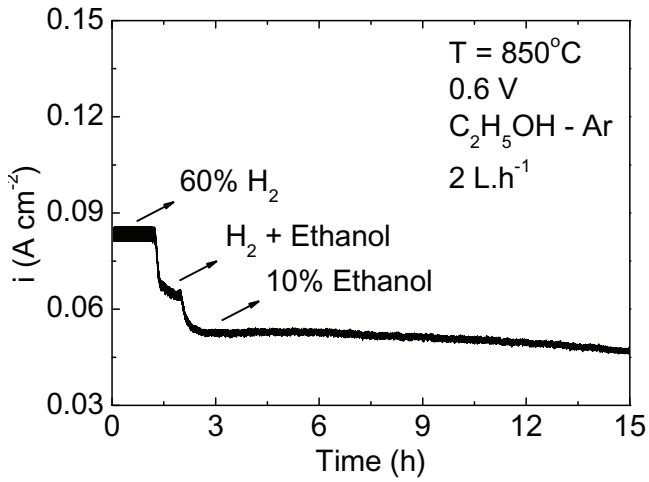

Fig. 5. Potentiostatic curve recorded at 850°C at 0.6 V for 10% ethanol, showing stable operation in dry ethanol for 12 h.

This observation gives a strong indication that ethanol was converted in the Ir-CGO catalytic layer into H_2, and no carbon formation occurred in the anode. Therefore, the Ir-CGO was demonstrated as an efficient catalyst for gradual internal reforming in a direct ethanol SOFC.

Using similar conditions, the stability in dry ethanol was tested for longer periods. Fig. 6 shows the polarisation curves during hydrogen and ethanol tests at 850°C. Fuel cell tests were initially performed in 60% H_2 balanced with 40% Ar, and a total flow of 4 $L.h^{-1}$. The polarisation curves were recorded from OCV to 0.4 V in H_2 and from 0.8 to 0.4 V in dry ethanol to ensure the GIR mechanism. The fuel flow rate was set to H_2:ethanol = 6:1. The results show comparable polarisation curves for hydrogen and ethanol adjusted for a constant theoretical number of electrons according to the simple mechanisms depicted in Fig. 1.

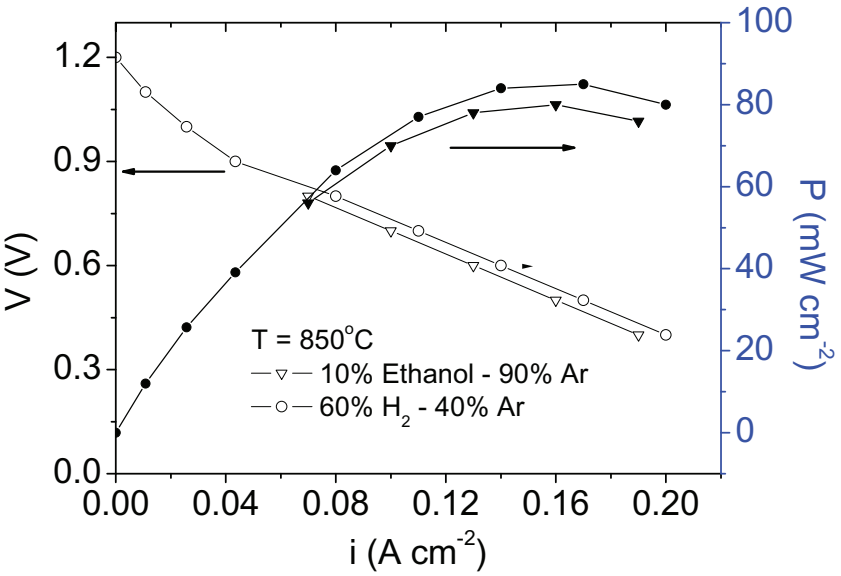

Fig. 6. Polarisation curves obtained at 850°C for H_2 and ethanol at 4 $L.h^{-1}$.

A potentiostatic test for 100 h was carried out. The time evolution of the current density is shown in Fig. 7. The operation at 0.6 V was initiated with H_2 balanced with Ar. After 10 min. the fuel was changed to dry ethanol. During 100 h, the single cell showed stable operation in 10% ethanol, at $i \sim 0.12$ $A.cm^{-2}$.

The stability of the current density observed for 100 hours is in good agreement with the first catalytic tests (not shown) in similar operation conditions at 850°C and with a ethanol:steam ratio of 1:3. The catalytic tests show that the reaction produces mainly hydrogen, CO and CO_2, with a small quantity of CH_4. Using pure CGO, without Ir, as the catalyst, the result is different. Several byproducts (ethylene, acetaldehyde, and methane) are detected. Such by-products strongly increase the risk of carbonaceous deposits and subsequent cell performance degradations.

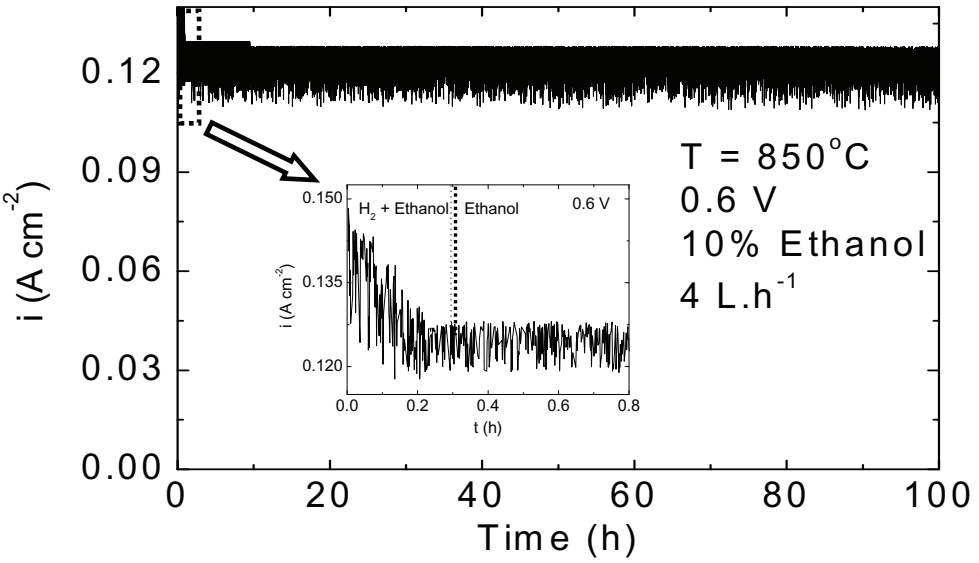

Fig. 7. Potentiostatic curve recorded at 850°C at 0.6 V for 10% ethanol.

4. Conclusions

The design and operation of electrolyte-supported single cells was described. An Ir-CGO catalytic layer allows the stable operation of the cell with dry ethanol. The stable operation of single cells is a significant evidence of the effectiveness of gradual internal reforming of ethanol. The presented results suggest that, provided that a suitable catalyst is available, along with an optimised cell design, solid oxide fuel cells can operate directly with carbon-containing fuels. Such results represent important progress, indicating that an SOFC can operate with an efficient renewable fuel. In addition, the combined results of both previously reported methane and presently ethanol open up the way for the development of multi-fuel solid oxide fuel cells.

Acknowledgments

The authors acknowledge CNEN, CNPq, CAPES (CAPES – COFECUB program) and ADEME for partial financial support and scholarships.

References

[1] X.F. Ye, S.R. Wang, Q. Hu, J.Y. Chen, T.L. Wen, Z.Y. Wen, Improvement of Cu-CeO_2 anodes for SOFCs running on ethanol fuels, *Solid State Ionics* 2009; **180**: 276–281.

[2] A. Erdohelyi, J. Rasko, T. Kecskes, M. Toth, M. Domok, K. Baan, Hydrogen formation in ethanol reforming on supported noble metal catalysts, *Catalysis Today* 2006; **116**: 367–376.

[3] H. Kan, H. Lee, Sn-doped Ni/YSZ anode catalysts with enhanced carbon deposition resistance for an intermediate temperature SOFC, *Applied Catalysis B: Environmental* 2010; **97**: 108–114.

[4] Z. Zhan, S.A. Barnett, Use of a catalyst layer for partial propane oxidation in solid oxide fuel cells, *Solid State Ionics* 2005; **176**: 871–879.

[5] N. Laosiripojana, S. Assabumrungrat, Catalytic steam reforming of ethanol over high surface area CeO_2: The role of CeO_2 as an internal pre-reforming catalysts, *Applied Catalysis B: Environmental* 2006; **66**: 29–39.
[6] N. Laosiripojana, S. Assabumrungrat, S. Charojrochkul, Steam reforming of ethanol with co-fed oxygen and hydrogen over Ni on high surface area ceria supporte, *Applied Catalysis A: General* 2007; **327**: 180–188.
[7] L.O.O. da Costa, A.M. da Silva, F.B. Noronha, L.V. Mattos, The study of the performance of Ni supported on gadolinium doped ceria SOFC anode on the steam reforming of ethanol, *Int. J. Hydrogen Energy* 2012; **37**: 5930–5939.
[8] I.A.C. Ramos, T. Montini, B. Lorenzut, H. Troiani, F.C. Gennari, M. Graziani, P. Fornasiero, Hydrogen production from ethanol steam reforming on M/CeO_2/YSZ (M = Ru, Pd, Ag) nanocomposite, *Catalysis Today* 2012; **180**: 96–104.
[9] L.J. Duhamel, C. Pirez, M. Capron, F. Dumeignil, E. Payen, Hydrogen production from ethanol steam reforming over cerium and nickel based oxyhydrides, *Int. J. Hydrogen Energy* 2010; **35**: 12741–12750.
[10] P. Vernoux, J. Guindet, M. Kleitz, Gradual Internal methane reforming in intermediate-temperature solid-oxide fuel cells, *J. Electrochem. Soc*. 1998; **145**: 3487–3492.
[11] J.M. Klein, Y. Bultel, S. Georges, M. Pons, Modeling of a SOFC fuelled by methane: From direct internal reforming to gradual internal reforming, *Chemical Engineering Science* 2007; **62**: 1636–1649.
[12] J.M. Klein, S. Georges, Y. Bultel, Modeling of a SOFC fueled by methane: anode barrier to allow gradual internal reforming without coking, *J. Electrochem. Soc*. 2008; **155**: B333–B339.
[13] J.M. Klein, M. Henault, P. Gelin, Y. Bultel, S. Georges, A solid oxide fuel cell operating in gradual internal reforming conditions under pure dry methane, *Electrochemical and Solid-State Letters* 2008; **11**: B144–B147.
[14] J.M. Klein, M. Hénault, C. Roux, Y. Bultel, S. Georges, Direct methane SOFC working by gradual internal steam reforming : analysis of operation, *J. Power Sources* 2009; **193**: 331–337.
[15] S.D. Nobrega, M.V. Galesco, K. Girona, D.Z. de Florio, M.C. Steil, S. Georges, F.C. Fonseca, Direct ethanol solid oxide fuel cell operating in gradual internal reforming, *J. Power Sources* 2012; **213**: 156–159 (in press).
[16] V. Esposito, D.Z. de Florio, E.N.S. Muccillo, R. Muccillo, E. Traversa, Electrical properties of YSZ/NiO composites prepared by a liquid mixture technique, *J. European Ceramic Soc*. 2005; **25**: 2637–2641.
[17] M. Wisniewski, A. Boréave, P. Gélin, Catalytic CO_2 reforming of methane over Ir/$Ce_{0.9}Gd_{0.1}O_{2-x}$, *Catal. Commun*. 2005; **6**: 596–600.